ONLINE ISSN :3007-309X
PRINT ISSN :3007-3081

Journal of Medical & Health Sciences Review

REMOVAL OF ARSENIC FROM FRESH WATER USING SUPERPARAMAGNETIC IRON OXIDE NANOPARTICLES SUPPORTED ON SULPHONATED SUGARCANE BAGASSE

Arif Ullah Khan[1*], Rabia Iqbal[2a], Qudsia Begum[3], Ayesha Siddiqa[2b], Iram Saba[4], Farheen Aslam[5], Shehzad Sikandar[6], Bisma Naeem[2c], Hameed Ur Rehman[7]

[1]Department of Chemistry, Kohat University of Science & Technology Kohat Khyber Pakhtunkhwa (KP) 26000, Pakistan, Email: arifmarwatulm@gmail.com

[2a,2b,2c] Institute of Microbiology and Molecular Genetics, University of the Punjab, Lahore Email: rabiarao084@gmail.com ayesha.mmg@pu.edu.pk bismanaeem2311@gmail.com

[3]Bahria University College of Allied Health Sciences, Bahria University Health Sciences Campus, Karachi Bahria University, Email: qudsiahameed93@gmail.com

[4]Department of Chemistry, Faculty of Natural Sciences, GC Women University Sialkot-51310, Pakistan, Email: iramsaba602@yahoo.com

[5]Department of Biotechnology, Lahore College for Women University, Email: farheenpu@gmail.com

[6]MPhil Scholar Department of Applied Chemistry, Government College University Faisalabad, Pakistan, Email: shehzadsikandar82@gmail.com

[7]Department of Elementary & Secondary Education Physical Education Teacher Government High School Teri, BD Shah Karak, KP, Pakistan, Email: 03449002451h@gmail.com

ARTICLE INFO

Keywords: Pomegranate Pulp Extract, Activated Carbon, Sugarcane Bagasse, Green Synthesis, UV-Visible Spectroscopy

Corresponding Author: Arif Ullah Khan, Department of Chemistry, Kohat University of Science & Technology Kohat Khyber Pakhtunkhwa (KP) 26000, Pakistan,
Email: arifmarwatulm@gmail.com

ABSTRACT

To synthesize superparamagnetic iron Oxide nanoparticles (SPIONS) by using pomegranate pulp extract. Activated carbon was made from sugarcane bagasse using a chemical impregnation process and then superparamagnetic iron oxide nanoparticle supported was on it. By using UV-visible spectroscopy, SEM, XRD and FTIR, the characterization of synthesized activated carbon (AC), SPION and Modified activated carbon (AC/SPIONs) were performed. According to the pictures of SEM, The synthesised Nanoparticles were spherical shape, more dispersed and it average ranges in size from 1nm-100nm. The functional groups and their physical interaction with SPIONs were showed in the FT-IR data. The XRD pattern demonstrated that the produced nanoparticles were crystalline. The majority of SPIONs were found to be attached to activated carbon's surface. The atomic absorption spectroscopy was used to analyze the activated carbon for adsorption of arsenic. The outcomes demonstrated that the arsenic ions adsorbed on the synthetic modified activated carbon best matched the Freundlich isotherm model, which predicted a heterogeneous distribution of active site over synthetic adsorbent and Physical adsorption. The Fruendlich constant (n), which indicates effective arsenic ion adsorption, was found to be greater than unity. Synthesised Modified activated carbon demonstrated significant adsorption and can be used for water purification.

INTRODUCTION

Because of its high toxicity and carcinogenicity, arsenic is a big issue in terms of human health and environmental pollution. Although natural events like volcanic eruptions and soil weathering release arsenic into the environment, but main cause of arsenic pollution is human beings [1].

The maximum arsenic discharge level was set by the World Health Organization (WHO) at 10 µg/L [2] but Unfortunately, in several countries' drinking water still contains levels of arsenic (As) greater than 50 µg/L. Due to high concentration of As, about more than 200 million people worldwide are exposed to unsafe level of As [3]. Arsenic in groundwater is found in two oxidation states: arsenate As[V] and arsenite As[III]. These species are found in groundwater in both inorganic and organic forms, with the inorganic forms being more toxic than the organic ones. Arsenic inorganic forms are approximately 100 times more toxic than organic species and are responsible for the majority of arsenic poisoning. Arsenate is approximately 60 times more toxic

than arsenite [4]. The most common diseases and side effects of arsenic poisoning are stomach pain, nausea, vomiting, diarrhoea, malfunctioning of the nervous and cardiovascular systems, skin, kidney, liver, and prostate cancers, and so on. Several technologies for removing arsenic from drinking water have been reported, including coagulation-flocculation, ion exchange, reverse osmosis, membrane filtration, and adsorption processes. Due to its low cost and high efficiency, adsorption has been widely used to remove arsenic from these materials [5, 6]. Because of their high selectivity for arsenic, iron oxides such as hematite and goethite have demonstrated good performance as arsenic adsorbents. However, due to their low mechanical resistance, iron oxides cannot be used in fixed bed columns [7, 8]. Since the last decade, arsenic removal has been investigated using low-cost adsorbents such as lignocellulosic materials and agricultural by-products. Agricultural by-products are of particular interest because they are produced in large quantities and are widely available worldwide. Sugarcane industries in Vietnam produce large amounts of sugarcane bagasse (SCB), which could be used to remove arsenic from water streams. The main components of SCB have been identified as cellulose (46.0%), hemicellulose (24.5%), lignin (19.5%), fat and waxes (3.5%), ash (2.4%), silica (2.0%), and others (1.7%) [9]. Sugarcane bagasse polysaccharides are biopolymers with many hydroxyl and/or phenolic groups that can be chemically modified to form new compounds with various properties [10]. Adsorbents that have been modified with iron oxides, such as activated carbon, have been reported in the literature to improve adsorption capacities and mechanical properties, indicating that arsenic adsorption processes are becoming more efficient [11, 12]. Adsorption is considered to be a practical and cost-efficient method for the removal of arsenic due to the lower cost, availability, and regeneration of suitable adsorbents. Although the adsorption capacity of agricultural by-products is typically lower than that of synthetic adsorbents, these materials could be a low-cost alternative for water treatment plants. These materials are modified with various organic compounds with different functional groups to increase their adsorption capacity. Biopolymers, primarily polysaccharides with hydroxyl, carboxyl, and/or phenolic groups, are found in SCB and can be chemically modified to form new compounds with different properties.

The purpose of this study is to look into the role and efficacy of nano-sized magnetic particles, specifically superparamagnetic iron oxide nanoparticles (SPION) supported on activated carban from waste biomass.

1. MATERIALS AND METHODS

Materials

To reduce the adsorption process's operating costs, waste biomass Pomegranate pulp and sugarcane bagasse were obtained from local juice shop. Concentrated H_2SO_4 (95–98%) and sodium hydroxide (> 97%) were purchased from Beijing Chemicals Company. $Na_2HAsO_4 \cdot 7H_2O$ and $FeSO_4 \cdot 7H_2O$ were purchased from Sigma–Aldrich. The adsorption mixture was homogenized using an ultrasonic bath sonicator (VWR 50 T). Deionized water from the lab's Milli-Q water purifier facilities (EMD Millipore Corporation) had a resistance of approximately 18.2M cm at 25 °C. The stock solutions of sodium arsenate heptahydrate were made in a standard volumetric flask (1000 mL).

Superparamagnetic Iron Oxide Nanoparticles Preparation (SPIONS)

Pomegranate pulp Obtained from a nearby juice shop as a low-cost source of agricultural waste. This pulp was first dried in an oven for 24 hours, then grinding and sieved through a 50-100 mesh. Then, 250 mL of pure distilled water was combined with 15 g of dried pomegranate powder. This mixture was thoroughly mixed at 150 rpm in an orbital shaker while being heated for one hour at 80 ºC. The solution was then brought to room temperature and vacuum-filtered to produce the extract. According to reports, citrus fruit extracts contain a variety of biomolecules, including flavonoids, alkaloids, antioxidants, and other phenolic compounds [13]. Additionally, these substances are said to be effective reducing agents[14], which reduce metal ions. $FeSO_4$ solution (5.8 mol/L) was added to the pomegranate pulp extract in a ratio of 1:3 (v/v) to synthesize SPIONs. When pomegranate pulp extract was added to iron solution. The solution color changed from brown to black. To adjust the solution PH, NaOH was added. Because of the addition of NaOH during this process, all metal ions were quickly converted into nano-metallic particles and the mixture turned black. Centrifugation was used to separate these particles. Then, the dark particles were dried in a vacuum for 24 hours at 60 ºC. Before being used again, the synthesized nanoparticles were calcined at 400 ºC for four hours and kept in a vacuum desiccator.

1.1 Activated Carbon synthesis

The sugarcane bagasse (SCB) was collected from juice shop in Kohat and put through a sieving device. A sieve fraction of 130–210 μm sample was carefully washed with deionized water for exclusion of contaminations, and dried in a ventilated oven at 65 ºC for 24 h.5g of Sugarcane bagasse mixed to 60ml Concentrated H_2SO_4 in rounded bottomed 300ml flask, to which a reflux condenser was attached. This reaction carried out for an additional hour while stirring as the

reaction mixture's temperature gradualy raised to H_2SO_4 boiling point. The experiment was carried out in a fume hood with adequate ventilation, wearing personal protective equipment, and taking extreme precautions. when the process of reflux was complete, to ambient temperature mixture of reacion was coolded and 4 °C of 260ml cold water gradually added while taking the necessary safety precautions. The excess H_2SO_4 was then removed from the product through vacum filteratig process and also through washing of deionized waer. Sulfonated SCB was then dried in a vacuum oven at 70 °C for 12 hours and grounded to fine powder using mortar and pestle. Activated carbon synthesis from sugarcane bagasse finally was collected and stored for later use.

2.4 Modified activated carbon preparation

Superparamagnetic iron oxide nanoparticles that were created through synthesis were combined with activated carbon in a ratio of 1:5 (w/w) to create modified activated carbon. Superparamagnetic iron oxide nanoparticle solution was mixed with one gram of activated carbon (0.2g superparamagnetic iron oxide nanoparticle, 80 ml deionized water). For 48 hours at room temperature, the solution was stirred using magnetic stirring. By filtering the product, modified activated carbon (AC/SPIONs) was produced. The resulting modified activated carbon was then dried at 60 °C for 24 hours after being washed three times with deionized water.

2.5 Batch adsorption experiment

In the 20 ml aqueous As(III) solutions of various concentrations, a defined amount of (0.2 g) modified activated carbon (AC/SPIONs) was added.10, 20, 40 , 60, 80, and 100 ppm dilutions from stock solution were prepared and shaken at 120 rpm for various time intervals using a rotary shaker (Retsch, Germany). Supernatant was filtered through a cellulose acetate filter (pore size 0.2 lm) and analyzed for As(III), using a “HG-AAS”. The mass balance of As(III) adsorbed per mass unit of the (AC/SPIONs) (mg/g) was calculated by the following (Eq. (1)) [15]:

$[Q_e= (C_i-C_e)V/W]$ (1) where “Ci” and “Ce” are the initial and equilibrium “As(III)” concentrations in mg/l, respectively. “V” is volume of the “As(III)” solution in ml, and “W” is the weight of adsorbent in mg.

3 Results and discussion

3.1 Study of uv-visible

Display of Absorbance of synthesized Superparamagnetic Iron Oxide Nanoparicle (SPIONs) is between 250 and 300 nm. At their typical wavelength of 275 nm, the nanoparticles displayed their highest absorbance. This value is much closer to the maximum absorbance for magnetic

nanoparticles previously reported at 280 nm. The other peaks are caused by the organic molecules that are stabilising organic molecules' absorbance. The extract displayed a potent 250 nm absorption band, which is a sign of aromatic amine and phenol[16]. Figure depicts the

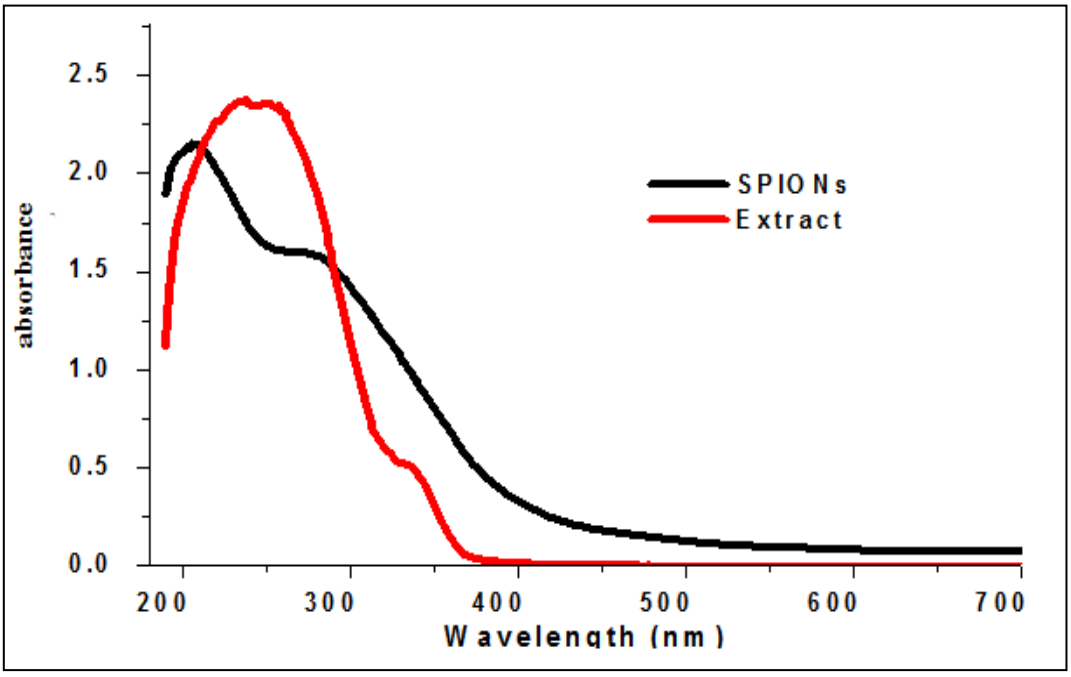

superparamagnetic iron oxide nanoparticles (SPIONs) and extract solution's UV-visible spectrum.

Fig: SPIONs UV-Visible spectra

Study of FT-IR

FT-IR spectroscopy was used to determine the Functional group of synthetic Activated Carbon, Superparamagnetic Iron Oxide Nanoparticles,and Modified Activated Carbon. The peak in activated carbon's region 2929 cm^{-1} is due to C-H stretching vibration. Likewise, the stretching vibration of the C=O group in a carboxylic acid is attributed to the band in the range 1728 cm^{-1}. Modified activated carbon (AC/SPIONs) has a bathochromic shift that exhibits this carbonyl group's distinctive stretching vibration band. The stretching vibration of O-H, which suggests the presence of a carboxyl group, is responsible for the broad band of extremely low intensity that is present between 3200 cm^{-1} and 3600 cm^{-1}. Modified activated carbon (AC/SPIONs) exhibits the stretching vibration of C=C with a shift to 1585 cm^{-1}, is attributed to the band in the region of 1596 cm^{-1}. In the specific region 1157 cm^{-1} of the C-O stretching vibration, activated carbon (AC) and modified activated carbon (AC/SPIONs) both exhibit it. With low intensity, modified activated carbon (AC/SPIONs) also exhibited the O-H group's stretching vibration, is attributed to the broad

band in superparamagnetic iron oxide nanoparticles (SPIONs) that is centred at 3350 cm^{-1}. The hydroxyl group's O-H stretching vibration mode is indicated by a shift in the absorption band from 3200 cm^{-1} to 3600 cm^{-1}, which suggests that the OH group is no longer necessary for activation of H_2SO_4. The bands in all of the spectra are in the range of 1250 cm^{-1} to 900 cm^{-1}, and the oxygenated functional groups are responsible for these vibrations. Finally, C-H stretching vibrations are assigned to the absorption bands in activated carbon at 2929 cm^{-1}. The peak in the vicinity of 544 cm^{-1} was given the Fe-O vibrational mode. In figure, the FT- IR spectra of Activated Carbon (AC), Modified Activated Carbon (AC/SPIONs), and superparamagnetic iron oxide nanoparticles (SPIONs) are displayed. Similar to this, the significant absorption bands and

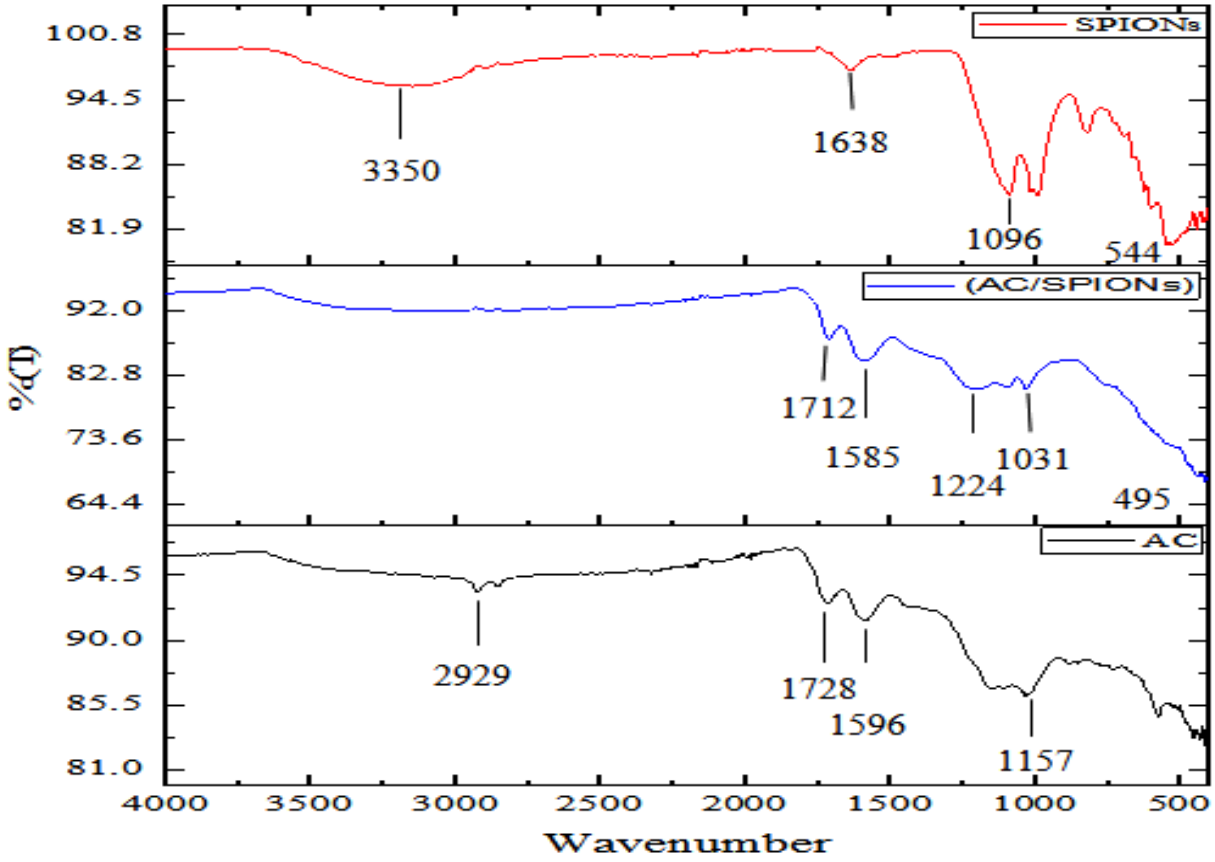

their assigned positions are displayed in the table.

Fig 2. : SPIONs, AC/SPIONs and AC FT-IR Spectra

Table; Main absorption data of FT-IR

S.No	IR signalcm^{-1}	Functional group	Assignment

1	3350	OH.	characteristic IR region of OH group.
2	2929	CH.	characteristic IR region of sp^3 CH
3	1710 - 1730	C= O	characteristic IR region of carbonyl group
4	1580 - 1600	C= C	characteristic IR region of C= C
5	1157	C- C	characteristic IR region of C- O
6	544	Fe- O	characteristic IR region of Fe- O

Study Of SEM

The size and surface morphology of the Synthesised Superparamagnetic Iron oxide Nanoparticles (SPIONs), Activated carbon (AC), and Modified Activated carbon (AC/SPIONs) were assessed using SEM images (as shown in Figure).. At 1kx magnification, a SEM image of prepared superparamagnetic iron oxide nanoparticles revealed both individual and accumulated nanoparticles with a sphere-shaped crystal structure. Sphere-shaped nanoparticles were typically 150 nm in size, but 200 nm particles were also observed. Accumulation of the particles is thought to be the cause of the particles' large size. According to SEM analysis, the produced nanoparticles are highly detached. Created activated carbon has a surface that is extremely porous with both small and large pores. As shown in figure, the surface is well-structured and waved, indicating that water and impurities were removed chemically by impregnation with H_2SO_4. Significant changes to the morphology, particularly in terms of size and pores, result from this chemical impregnation. Sometimes, the intrinsic properties of pure activated carbon are insufficient to effectively remove the contaminants. As a result, processes for altering activated carbon may be used. Many changes are made to activated carbon, including the addition of nanomaterials to increase its sorption capacity. [17].

Increased pore volumes and specific surface areas are just two examples of the modified activated carbon's improved properties.

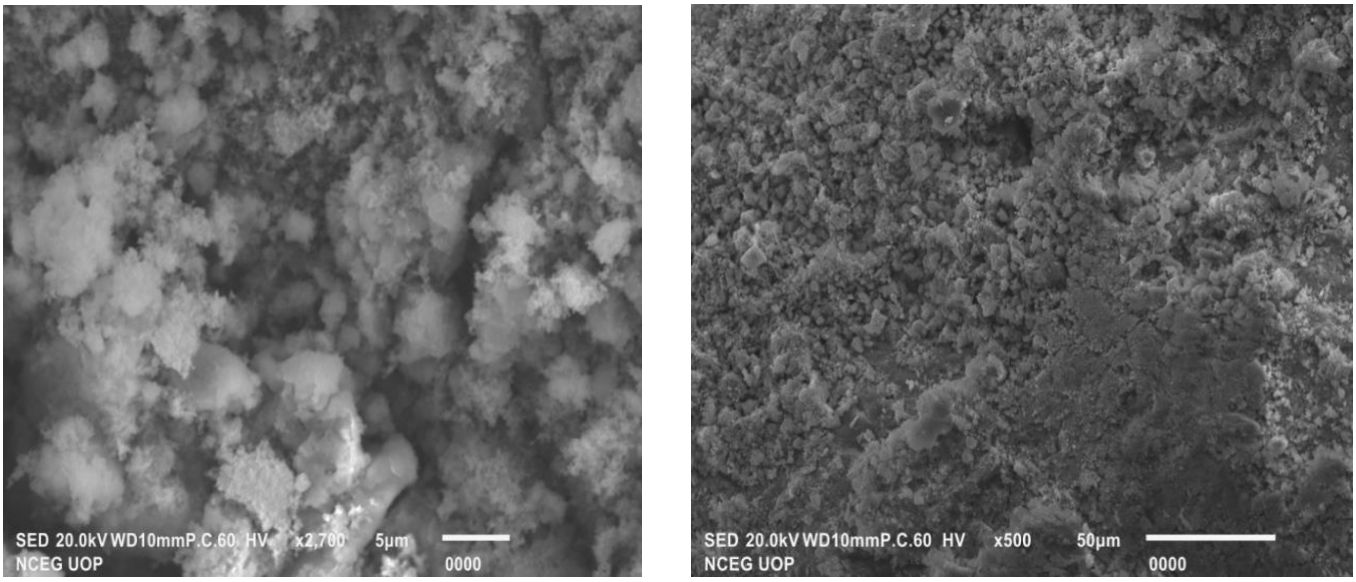

Fig: SEM images of synthesized SPIONs

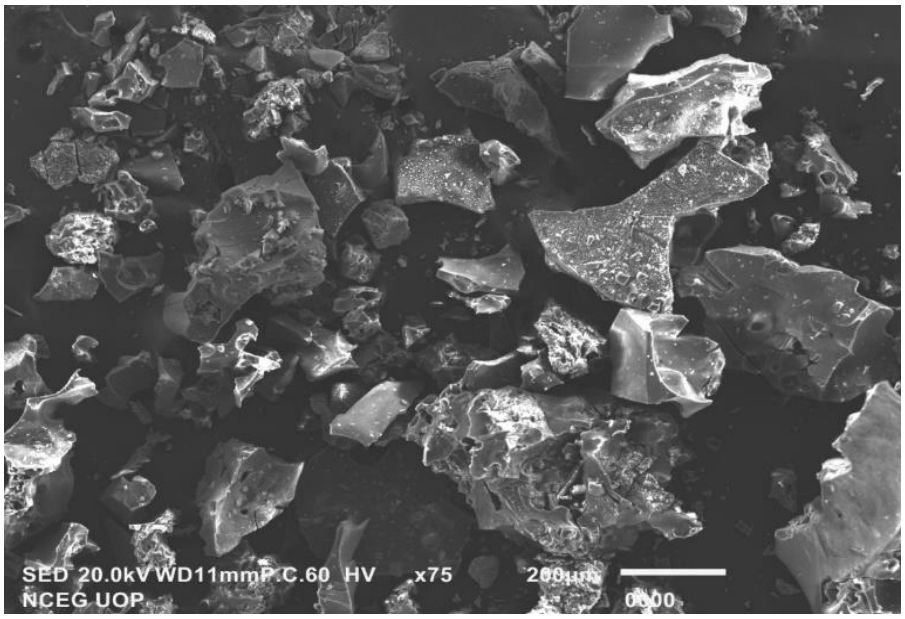

Fig; SEM image of activated carbon

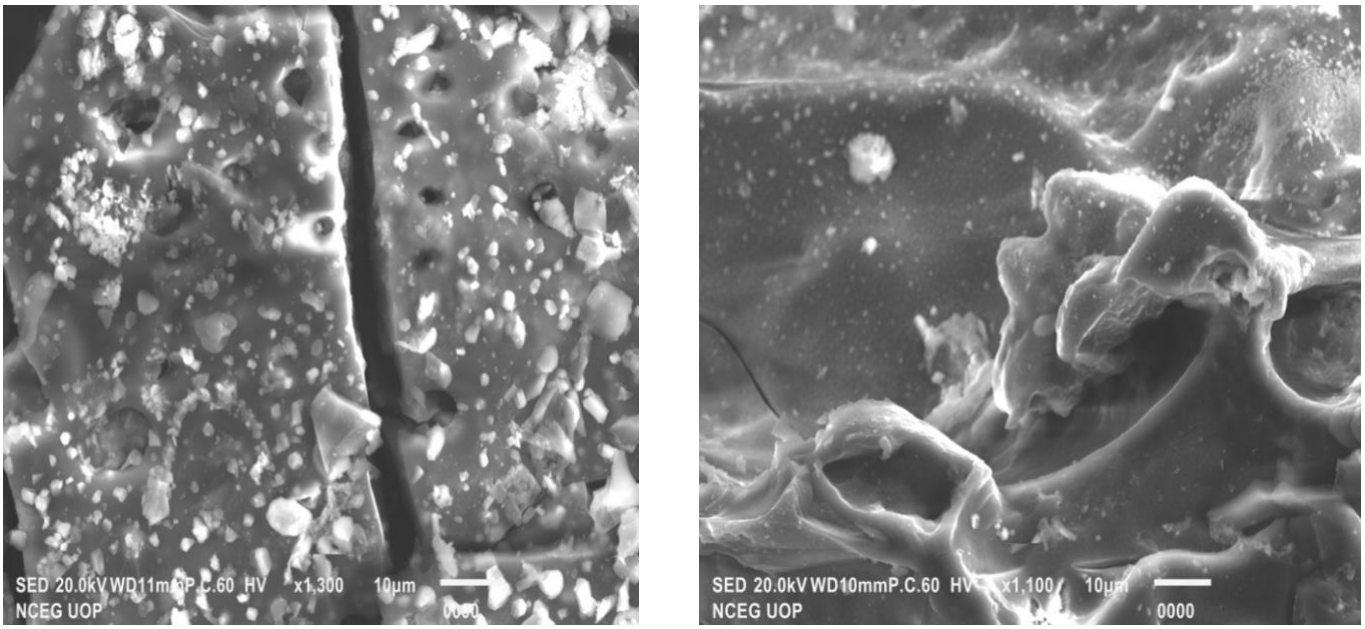

Fig: Modified Activated Carbon SEM micrographs

Study of XRD

As shown in Fig. 1, XRD analysis of SPOINs, modified activated carbon, and AC (AC/SPOINs) was conducted. Synthesized magnetic iron oxide nanoparticles' x-ray diffraction pattern revealed five noticeable Reflection lines at [2θ = 30. 45°, 35. 55°, 42. 4°, 57. 15° and 62. 15° corresponding to (2 2 0), (3 1 1), (4 0 0), (5 1 1) and (4 4 0) respectively]. There are no peaks for the hematite phase in the diffraction pattern, which indicates that the peak positions are indicative of the magnetite phase. A cube-shaped structure was recommended to match the JCPDS reference number 19-629. The peak intensities showed that there are no impurities in the SPIONs' crystalline structure. Two broad peaks around 2 = 23° and 43°, which are the distinguishing features of amorphous activated carbon, were seen in the case of Activated carbon. These peaks indicated micro-crystallites that resembled graphite and were randomly oriented in the (0 0 2) and (1 0 0) planes. Other low-intensity peaks that are seen could be inorganic salts. Figures a, b, and c show the XRD patterns of modified activated carbon, superparamagnetic iron oxide nanoparticles, and unmodified activated carbon. Similarly, Modified activated carbon (AC/SPOINs) was found to have an XRD pattern with a little peak position change. SPOINs and AC's XRD patterns were compared, and the results indicated that both samples contained crystalline nanoparticles. The Nanoparticle existance upperly attached on Activated carbon which is was also confirmed by the discovery of a broad diffraction hump with extremely low intensity

at 2 θ of 23°. According to the Scherer equation, the crystal size of both magnetite nanoparticles was range from 125nm to 130 nm.

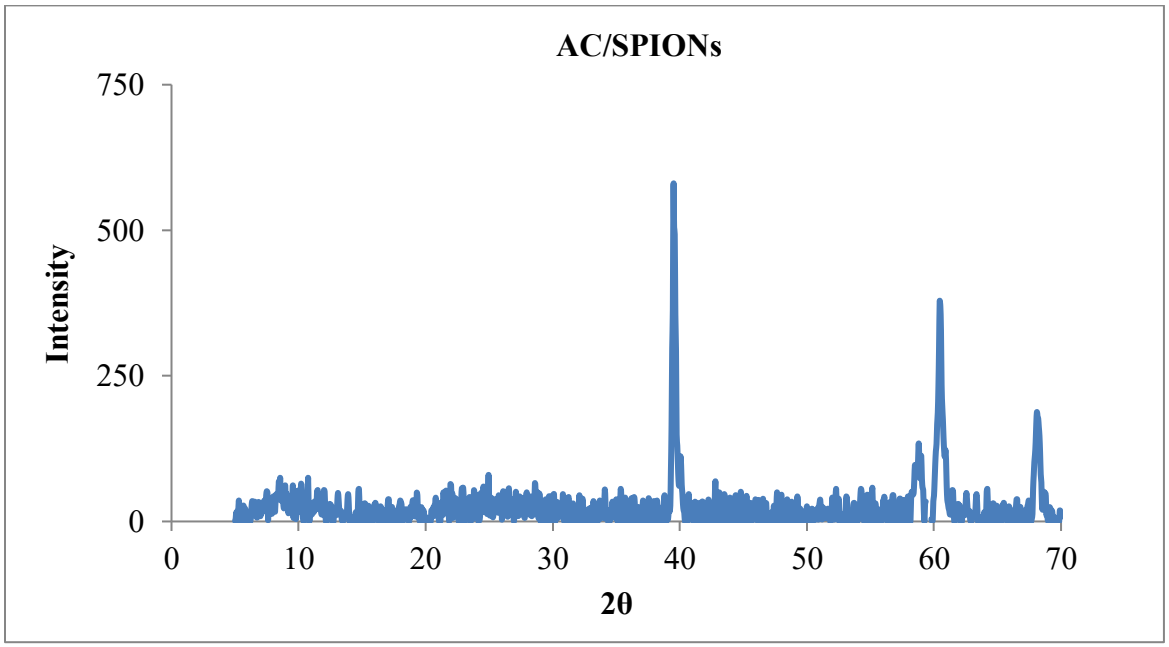

Fig a; SPIONS XRD Pattern

Fig b; Modified Activated Carbon (AC/SPIONs) XRD Pattern

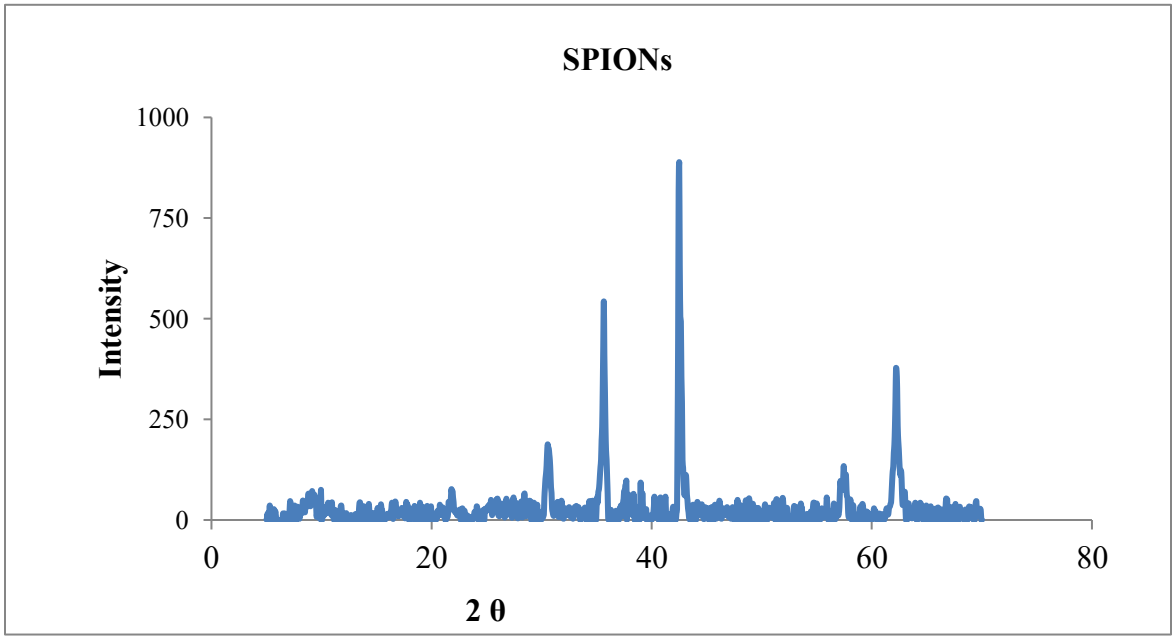

Fig c; Activated Carbon (AC) XRD Pattern

Study of Arsenic adsorption by AAS

Adsorption process was used to study the removal of arsenic, and atomic absorption spectroscopy was used for analysis. In order to achieve satisfactory performance, various adsorption conditions

were studied for the modified activated carbon with Superrparamagnetic Iron Oxide Nanopartiicle. Superparamagnetic iron oxide nanoparticles made synthetically increase the sponginess and superficial area for the adsorption of Arsenic ions. Calculations using atomic absorption spectroscopy were used to determine the percentage of arsenic ions that adhered to modified activated carbon for various initial concentrations.

Adsorption Isotherm.

The adsorption study explains how the adsorbate (arsenic ion) interacts with the adsorbent (AC/SPIONs) and how metal ions in solution achieve equilibrium during adsorption on surface. A variety of hypotheses, the majority of which are connected to the type of surface coverage i.e are supported by the adsorption isotherm, which shows how different adsorbate species are distributed between liquid and adsorbent. i.. Different adsorbate species may interact, and the adsorbent can be homogeneous, heterogeneous, multilayer, or monolayer. Atomic absorption spectroscopy was used in this study to obtain the adsorption equilibrium data, which were then fitted into the Langmuir and Freundlich adsorption isotherm using modified activated carbon as the adsorbent and arsenic ion as the adsorbate.

Langmuir Adsorption Isotherm

The Langmuir adsorption isotherm states that the maximum adsorption of a species is related to the saturation of a monolayer of adsorbate species on the adsorbent surface, after which no additional adsorption takes place. Because there is no adsorbate diffusion on the surface of the adsorbent and the surface of the adsorbent has an even energy distribution, the isotherm accurately represents adsorption.

This Equation represents the Langmuir's Adsorption model.

$$\frac{C_e}{q_e} = \frac{1}{q_m K_L} + \frac{C_e}{q_m}$$

where qe is the equilibrium adsorbed metal content (mg/g), Ce is the equilibrium metal ion concentration (mg/L), The "K_L" Langmuir isotherm constant "L/mg" is a measurement of the adsorption free energy and the maximum monolayer adsorption capacity is "qm" (mg/g). The slop and intercept of the plot of Ce/qe versus Ce are used to calculate KL and qm.

Freundlich Adsorption Isotherm

The Freundlich isotherm for multilayer adsorption describes the adsorbate's random and asymmetric distribution over the surface plan. Equation depicts the Freundlich model.

$$\log q_e = \log K_F + 1/n(\log C_e)$$

where "KF" is the adsorption capacity and n is the adsorption strength. The intercept and slop of the plot of "log qe" versus "log Ce" are used to calculate KF and n. The parameters for the Langmuir and Freundlich isotherm models are presented in the table and respectively. Figure depicts similar Langmuir and Freundlich isotherms for synthetically produced modified activated carbon (AC/SPIONs) with varying As(III) ion concentrations. According to experimental results for the Langmuir and Freundlich isotherms, the determination coefficient values "R^2" were determined and are shown in the table. According to the data, the Freundlich isothermal model, which proposed a heterogeneous distribution of active sites across synthetic and physical adsorbents, best describes the adsorption of As(III) ions on synthesis modified activated carbon (AC/SPIONs). Freundlich and Langmuir isotherms have correlation coefficients "R^2" of 0.998 and 0.89, respectively. As(III) ions may adhere well to manufactured modified activated carbon since the Freundlich constant (n) for the experimental results is larger than unity.

Table ; Parameters of Langmuir Isotherm for "As(III)" ions removed by "AC/SPIONS"

C_e (mg/L)	q_e (mg/g)	C_e/q_e
0.057	1.86	0.030
1.24	3.49	0.355
5.44	6.29	0.864
12.56	9.83	1.277
21.58	11.68	1.847
35.45	14.27	2.482

Fig; Langmuir adsorption isotherm for ‘As(III)’ onto ‘(AC/SPIONS)’

Table; Freundlich isotherm parameters for ‘As(III)’ ions removel by ‘(AC/SPIONS)’

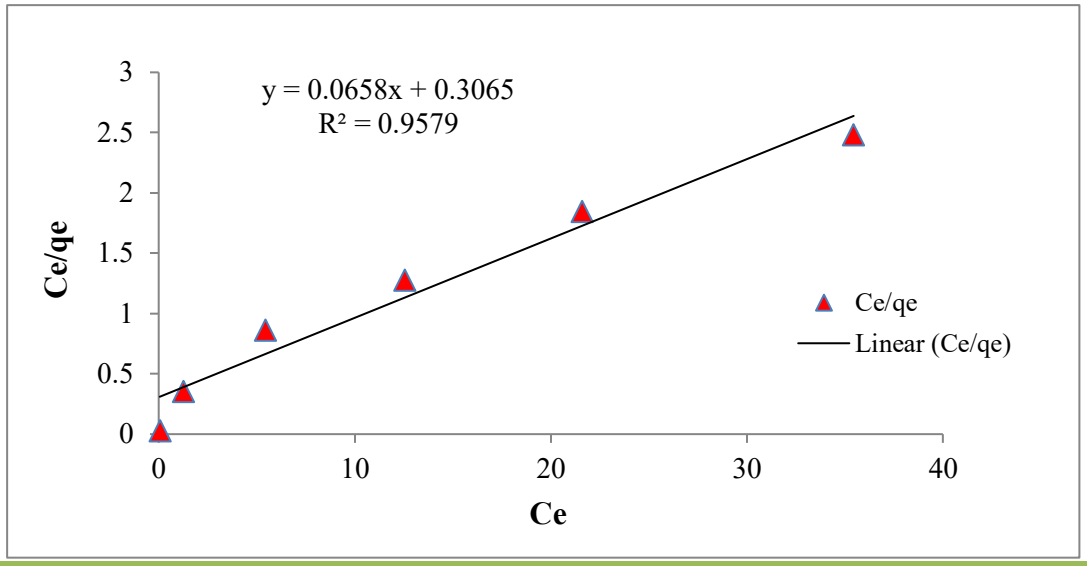

Ci (mg/L)	Ce (mg/L)	Log Ce	qe (mg/g)	Log qe
10	0.67	-0.17393	1.86	0.269513
20	2.51	0.399674	3.49	0.542825
40	8.52	0.93044	6.29	0.798651
60	15.85	1.200029	9.83	0.992554
80	21.58	1.334051	11.68	1.067443
100	28.61	1.456518	14.27	1.154424

Figure; Freundlich adsorption isotherm of 'As(III)' ions onto '(SPIONS)'

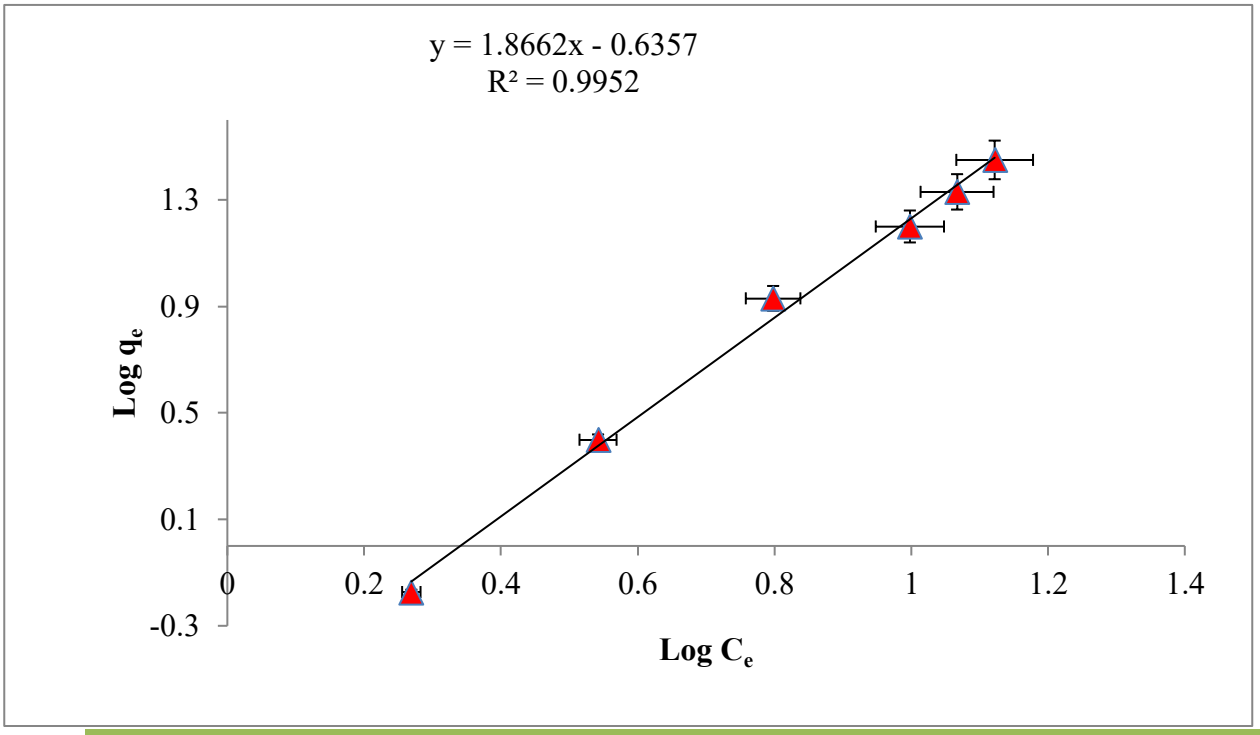

Langmuir			Freundlich		
R^2	q_m (mg/g)	K_L (L/mg)	R^2	K_F	1/n
0.957	15.38	51.26	0.995	0.643	1.866

Table; Freundlich and Langmuir isotherms parameters

The adsorption isotherms show that the modified activated carbon demonstrated significant adsorption capacity across the entire range of arsenic concentrations studied under ideal experimental conditions. The shape of the adsorption isotherm shows that the synthesised modified activated carbon (AC/SPIONs) had a high affinity for As(III) ions at low concentration. This is the desired quality of an adsorbent that will be used to treat arsenic-polluted water because the concentration of arsenic in the arsenic-contaminated areas does not exceed 1.5 ppm. Our synthesized modified activated carbon (AC/SPIONs) has an equilibrium adsorption capacity of 18.5 mg As/g for a solution containing 20 ppm of arsenic. The superior adsorption capacity of the material is correlated with the availability and particle size of the synthetic iron oxide nanoparticles

loaded onto activated carbon. The higher As(III) capacity noted in this study indicates that the adsorbents may have potential for use in arsenic removal.

4.8 Effect of concentration of As(III) ions on % adsorption

The adsorption investigation, according to published research, was carried out at a pH of 7. A graph of the initial As(III) ion concentrations versus the amount of metal adsorbed and the percentage of adsorption can be seen in Figure 4.8. When the concentration of As(III) ions was increased from 20 ppm to 100 ppm, as the adsorption percentage decreased to 71.3%, it was discovered that the amount of As(III) ions in the aqueous solution and the amount adsorbed were linearly related. The direct interaction of surface porosity and homogeneity with ions provides an explanation for this. The decrease in adsorption capacity can be attributed to the As(III) ions' inability to bind to all of the available sites as their concentration rises because the amount of adsorbent (AC/SPIONs) remained constant. The number of available sites decreases as adsorption sites become saturated. The literature for Fe modified activated carbon indicates a decreasing trend in the percentage As(III) adsorption with concentration. Our artificially created modified activated carbon (AC/SPIONs) can effectively remove As(III) from contaminated water with a maximum contamination limit of 1.5 mg/L at neutral pH.

Table; Initial As(III) concentrations effect on its adsorption

Concentration (ppm)	C_e	Adsorption '%'	q_e (mg/g)
10	0.057	93.3	1.86
20	1.24	87.45	3.49
40	5.44	78.7	6.29
60	12.56	73.58	9.83
80	21.58	73.0	11.68
100	35.45	71.3	14.27

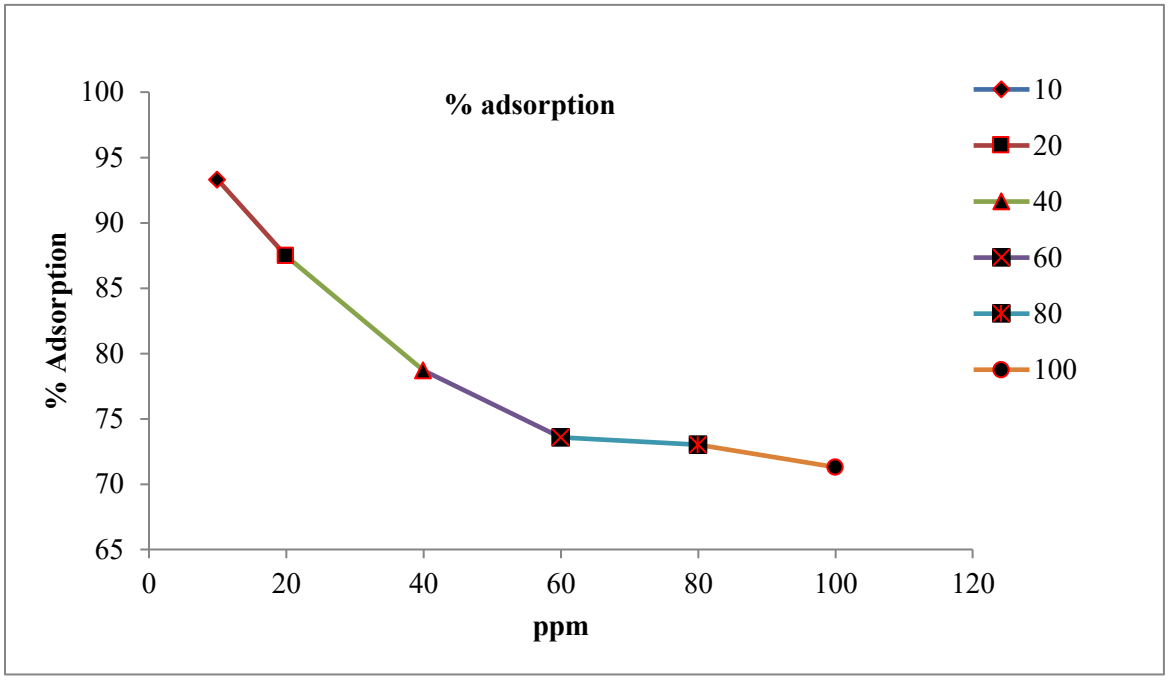

Fig : Intial concentration effect on adsorption

Conclusion

Modified activated carbon (AC/SPIONs) was made by combining superparamagnetic iron oxide nanoparticles with activated carbon derived from sugarcane bagasse. The characterization methods of XRD, SEM, UV-Vis, and FT-IR all supported the formation of modified activated carbon (AC/SPIONs), superparamagnetic iron oxide nanoparticles, and activated carbon. The nanoparticles were observed to be between 1nm and 100 nm. Using modified activated carbon as an adsorbent material, batch adsorption experiments were conducted to remove As (III) ions from aqueous solution. At pH 7 and 25 C, the Modified Activated Carbon (AC/SPIONs) was found to have excellent As (III) adsorption capacity. The equilibrium findings from this investigation fit the Freundlich isotherm more closely than the Langmuir isotherm. It showed that multilayer adsorption of arsenic took place on the modified activated carbon's (AC/SPIONs) heterogeneous surface. Based on comparisons of maximum adsorption capacity with previously investigated adsorbents, the magnetic composite synthesized in this work was found to be an efficient adsorbent for the adsorptive removal of As (III) from aqueous solution. So, the sugarcane bagasse-based

magnetic composite adsorbent showed significant promise for the adsorptive removal of As (III) from aqueous solution.

References:

[1] M. Z. Alam, M. Hoque, G. J. Ahammed, R. McGee, and L. Carpenter-Boggs, "Arsenic accumulation in lentil (Lens culinaris) genotypes and risk associated with the consumption of grains," *Sci Rep,* vol. 9, no. 1, pp. 1-9, 2019.

[2] A. K. Shakya and P. K. Ghosh, "Simultaneous removal of arsenic, iron and nitrate in an attached growth bioreactor to meet drinking water standards: importance of sulphate and empty bed contact time," *Journal of Cleaner Production,* vol. 186, pp. 1011-1020, 2018.

[3] F. Castriota *et al.*, "Chronic arsenic exposure impairs adaptive thermogenesis in male C57BL/6J mice," *American Journal of Physiology-Endocrinology and Metabolism,* vol. 318, no. 5, pp. E667-E677, 2020.

[4] C. Jain and I. Ali, "Arsenic: occurrence, toxicity and speciation techniques," *Water research,* vol. 34, no. 17, pp. 4304-4312, 2000.

[5] D. Mohan and C. U. Pittman Jr, "Arsenic removal from water/wastewater using adsorbents—a critical review," *Journal of hazardous materials,* vol. 142, no. 1-2, pp. 1-53, 2007.

[6] M. Vaclavikova, G. P. Gallios, S. Hredzak, and S. Jakabsky, "Removal of arsenic from water streams: an overview of available techniques," *Clean Technologies and Environmental Policy,* vol. 10, no. 1, pp. 89-95, 2008.

[7] X. Guo, Y. Du, F. Chen, H.-S. Park, and Y. Xie, "Mechanism of removal of arsenic by bead cellulose loaded with iron oxyhydroxide (β-FeOOH): EXAFS study," *Journal of colloid and interface science,* vol. 314, no. 2, pp. 427-433, 2007.

[8] A. V. Vitela-Rodriguez and J. R. Rangel-Mendez, "Arsenic removal by modified activated carbons with iron hydro (oxide) nanoparticles," *Journal of environmental management,* vol. 114, pp. 225-231, 2013.

[9] L. Sene, A. Converti, M. Felipe, and M. Zilli, "Sugarcane bagasse as alternative packing material for biofiltration of benzene polluted gaseous streams: a preliminary study," *Bioresource technology,* vol. 83, no. 2, pp. 153-157, 2002.

[10] E. Pehlivan, H. Tran, W. Ouédraogo, C. Schmidt, D. Zachmann, and M. Bahadir, "Sugarcane bagasse treated with hydrous ferric oxide as a potential adsorbent for the removal of As (V) from aqueous solutions," *Food chemistry,* vol. 138, no. 1, pp. 133-138, 2013.

[11] W. Chen, R. Parette, J. Zou, F. S. Cannon, and B. A. Dempsey, "Arsenic removal by iron-modified activated carbon," *Water research,* vol. 41, no. 9, pp. 1851-1858, 2007.

[12] V. Fierro, G. Muñiz, G. Gonzalez-Sánchez, M. Ballinas, and A. Celzard, "Arsenic removal by iron-doped activated carbons prepared by ferric chloride forced hydrolysis," *Journal of Hazardous Materials,* vol. 168, no. 1, pp. 430-437, 2009.

[13] C. B. Murray, C. R. Kagan, and M. G. Bawendi, "Synthesis and characterization of monodisperse nanocrystals and close-packed nanocrystal assemblies," *Annual review of materials science,* vol. 30, no. 1, pp. 545-610, 2000.

[14] L. Xiao, Y. Qiao, Y. He, and E. S. Yeung, "Three dimensional orientational imaging of nanoparticles with darkfield microscopy," *Analytical chemistry,* vol. 82, no. 12, pp. 5268-5274, 2010.

[15] T. Altun and E. Pehlivan, "Removal of Cr (VI) from aqueous solutions by modified walnut shells," *Food Chemistry,* vol. 132, no. 2, pp. 693-700, 2012.

[16] L. Li *et al.*, "Superparamagnetic iron oxide nanoparticles as MRI contrast agents for non-invasive stem cell labeling and tracking," *Theranostics,* vol. 3, no. 8, p. 595, 2013.
[17] M. Aremu, A. Arinkoola, I. Olowonyo, and K. Salam, "Improved phenol sequestration from aqueous solution using silver nanoparticle modified Palm Kernel Shell Activated Carbon," *Heliyon,* vol. 6, no. 7, p. e04492, 2020.